QUASIELASTIC LIGHT SCATTERING FROM MIGRATING CHEMOTACTIC BANDS OF *ESCHERICHIA COLI*

II. ANALYSIS OF ANISOTROPIC BACTERIAL MOTIONS

PAUL C. WANG AND SOW-HSIN CHEN, *Nuclear Engineering Department, Massachusetts Institute of Technology, Cambridge, Massachusetts 01239*

ABSTRACT Chemotactic effects of dissolved oxygen on motions of Escherichia coli in a motility buffer solution have been studied by measurements of quasielastic light scattering. Under conditions where the bacteria form a sharp band in an oxygen concentration gradient created by their metabolism, components of motions along the direction of the gradient and perpendicular to it were studied separately at each point within the band profile. A theoretical model for bacterial self correlation function based on two-state motions has been developed to extract the mean square speed of run motion and the relative probability of twiddle vs. run at each point of the band profile. A combined novel experimental set-up and new data analysis method allowed us to extract also the mean square displacements at short times along and perpendicular to the direction of the gradient. Parameters extracted from the measured correlation functions have been discussed in the framework of the established picture of bacterial motions under chemotaxis.

INTRODUCTION

Microscopic motions of individual *Escherichia coli* in liquid chemotactic media have been extensively studied by stroboscopic photomicrographs (1) and especially by tracking microscope (2). These techniques work well when bacterial density in solution is relatively low. The motions were shown to be characterized by two states: either a "running" state in which a bacterium moves in a fairly straight path or a "twiddle" state in which the bacterium jigs around locally. In a homogeneous medium the twiddle occurs with a constant probability. A twiddling bacterium will then make a run in a new randomly chosen direction and the sequence of the motions repeats. However, in the case of chemotaxis the random walk of the bacterium is biased toward the chemical gradient by lowering the frequency of twiddle in that direction (3–5). In a favorable direction a bacterium tends to run longer and twiddles less frequently. Thus, on the average there is a net displacement in this favorable direction. In a motility buffer saturated with oxygen, the metabolic activity of bacteria creates a traveling oxygen concentration gradient, which the bacteria follow collectively (6). This collective motion results in formation of a traveling band that we call a chemotactic band. Bacterial density in a chemotactic band is typically as high as 10^8/ml. Under this condition neither technique mentioned above (1,2) applies.

In our previous experiment (7), which we shall refer to as experiment I from now on, we measured the average isotropic motions of *E. coli* in the chemotactic band by quasielastic light

scattering. Specifically, we study halfwidths of the self-correlation functions at different scattering angles. The halfwidth vs. scattering angle (θ) plot clearly showed that while at small θ contributions to the width come from both running and twiddling, at large θ it is mainly determined by the running motion. We developed in experiment I a model that takes both the twiddling and running motions into account and we showed that with a reasonable choice of parameters the model produces self correlation functions that agree well with the measurements at all angles. This agreement at large angles may be fortuitous because it has been shown (8,9) that at large scattering angles the contribution from "wobbling" motions during the run become significant. As a result the fitted parameters (7), especially β which measures the relative probability of twiddle versus run, may be in error. Furthermore, owing to the necessity of performing measurements at all angles, which take more than an hour each time, the correlation functions measured were those averaged over the whole band.

In this second report, we wish to study the average motion of bacteria in different portions of the chemotactic band, or more specifically, components of motions of a bacterium in directions parallel and perpendicular to the chemical gradient. For this purpose, a computer-controlled data acquisition system is set up. This set up can store data in a cassette tape of the computer within two and a half minutes. Using this, we are able, for the first time, to study the bacterial motions at different portions of the migrating band with a spatial resolution of ~ 100 μm. As the band passes through the beam, the self-correlation functions at each consecutive section of the band are obtained. Two scattering vectors, one parallel and the other perpendicular to the direction of oxygen concentration gradient, are used to study the bacteria

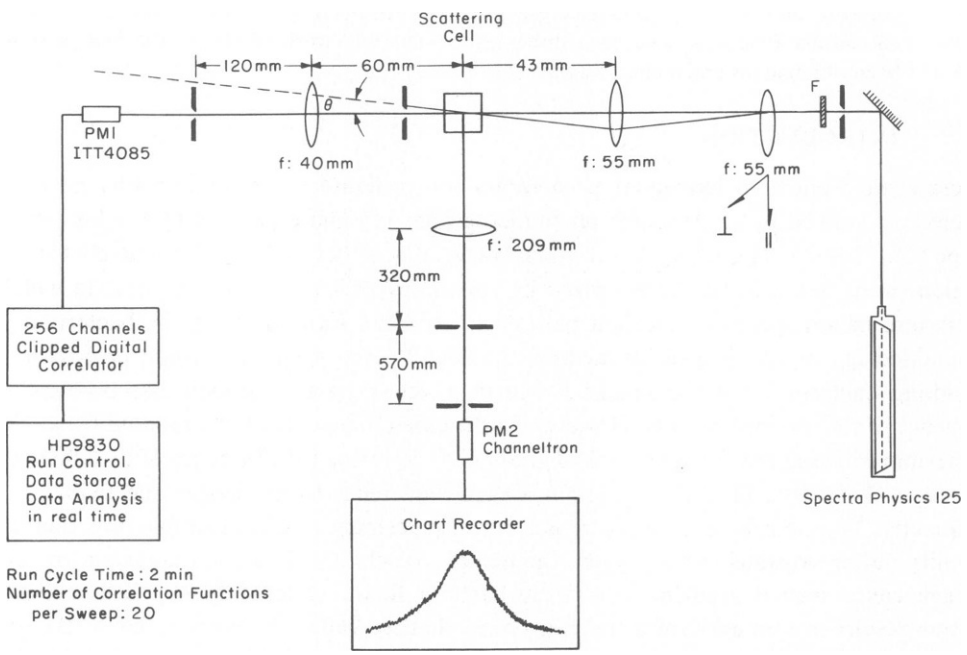

FIGURE 1 Schematic diagram of the photon correlation spectrometer. By moving the first two lenses on the right hand side up and down or right and left, one can bend the incident beam downward and sideways. These movements are used to direct the scattered vector parallel or perpendicular to the oxygen concentration gradient.

motions in these directions. To minimize effects due to nonspherical shape and internal structure (10) of bacteria, and also to the wobbling motions (9) on the measured correlation functions, we chose to measure the correlation function at two small angles: 3.72° and 8.67°. Another measurement at 90° serves as a reference point for comparison with previous experiments (7). The scaled halfwidths of the self-correlation functions around the center of the band are found to be significantly narrower than those from the leading and tailing edges in the parallel case. In contrast, widths of the self-correlation functions hardly vary throughout the whole band in the perpendicular case.

In this paper we also introduce a new method of data analysis. We extended the model developed in experiment I to take into account transition from one state to another. As a result we are now able to extract from the correlation functions the average speed of run motion, the average run time, and the relative probability to twiddle vs. run at given portion of the band. When these parameters are compared for motions parallel and perpendicular to the gradient some interesting features begin to emerge. Using these parameters, we also calculate the mean-square displacement as a function of time. It gives some physical insight about the motion of the bacterium at short times. The mean-square displacement in the parallel direction is found to be significantly larger than that in the perpendicular direction. We have now demonstrated for the first time that the quasielastic scattering of light can be used effectively for measuring relevant parameters for bacteria in a chemotactic band.

EXPERIMENT

Sample Preparation

Bacteria *E. coli* K12 wild type are grown in L-broth for 4h at 37°C in shaking scheme to the mid-log phase. The scattering cell (vol 8 cm^3, cross section 2 cm^2) is first rinsed and filled with motility buffer (10^{-2}M) KH_2PO_4, pH 6.9, 10^{-4}M EDTA and 10^{-6}M L-methionine) (9). Then 250 μl of the culture medium is carefully injected at the bottom of the scattering cell by a syringe. Density of bacteria in the culture medium is $\sim 1 \times 10^8$/ml. After 10–20 min a 1-mm thick band containing highly motile bacteria appears on the top of the inoculant. Bacterial density in the center of the band is $\sim 1 \times 10^8$/ml. The band migrates upward slowly following the oxygen concentration gradient that is created by the metabolic activity of the bacteria. The migrating speed of the band slows down slightly along the path. It changes from 0.85μm/s at 1 h after inoculation to 0.45μm/s at 5 h after the inoculation.

Scattering Setup

The photon correlation spectrometer is schematically shown in Fig. 1. It is similar to a setup previously used in this laboratory (7,12). Laser light (Spectra Physics 125 Å He-Ne laser; Spectra-Physics Inc., Mountain View, Calif.) of wavelength 6,328 Å was focused and bent by two lenses L_1 (f = 55 mm) and L_2 (f = 55 mm). It passes through the center of the scattering cell with a focused beam diameter of ~ 6.7μm at power level of 30 mW. The typical photon counting rate at small scattering angles is ~ 4,000 cps at the center of the migrating band.

To measure scattering in the forward direction the following device is used. By adjusting lenses L_1 and L_2 up and down or sideways, the scattering vector can be chosen either parallel or perpendicular to the direction of the migrating band at the desired small angle. A set of neutral density filters was used for attenuating the incident intensity of the laser beam. At scattering angle of 3.7° and bacterial density 10^8/ml, the scattering volume is estimated to be 3×10^{-6} ml. Thus there are about 340 bacteria in the scattering volume. At the larger scattering angle 8.7°, the corresponding number of bacteria is 62. Under this condition, because of the small number of bacteria in the scattering volume, we do not have to be concerned about the number fluctuation effect. Since the collimation is very tight on the scattering side

the narrowing effect of the correlation function from multiple scattering is negligible. Thus with a typical band migration speed of 0.85μm/s, the band itself scans through the beam in ~ 20 min.

The 256-channel photon correlator constructed in our laboratory (10) is interfaced with a Hewlett-Packard 9830/A calculator (Hewlett-Packard Co., Palo Alto, Calif.) via a Tracor Northern NS-570 multi-channel analyzer (MCA) (Tracor Northern, Middleton, Wis.). In a typical measurement loop, the computer sends a pulse to start the MCA. After a period of data accumulation (normally 2 min) the computer sends a signal to stop MCA and initiate data transfer from MCA to the computer memory and then onto a cassette tape. This step takes 30 s. Immediately after the completion, the computer resets the MCA and restarts the data accumulation. While the MCA is accumulating data, the computer estimates the uncorrelated background, calculates the normalized self-correlation function, estimates its halfwidth and prints out the self correlation function also. The uncorrelated background is taken to be proportional to the scattered intensity which is used to obtain the band profile. The mean-square displacement and further detailed analysis of the self-correlation function are done after the experiment from the recorded data.

Data Processing

To normalize the self-correlation function, the correlation function at zero delay time is obtained by an extrapolation. The second to ninth channel data are used for this purpose by a least-square fitting to a parabola. The first channel data are not used to avoid the danger of their being contaminated by after-pulsing effect of the photomultiplier tube. The average value of data from the last 20 channels is used as an estimate of the uncorrelated background. After subtraction of the background, the square roots of the normalized data, which are normalized to the zeroth channel, are taken to be the self-correlation function. The halfwidth was found from a 10 points weighted least-square fitting centered at a rough estimated halfwidth channel.

THEORY

In the case of chemotaxis we are interested mainly in the center of mass motion of bacteria. Since the physical dimension of *E. coli* is comparable to the wavelength of light used in the light scattering experiment and since *E. coli* bacteria are not spherical particles, the correlation function measured reflects, in general, the size and the shape effects besides the center of mass motion. It has been shown (13) that the so-called Rayleigh-Gans approximation is applicable in the case of light scattering from *E. coli* and that under this approximation the finite size and shape effects are negligible whenever a criterion $qd < 1$ is satisfied (14). Here d is the typical dimension of *E. coli* and q is the magnitude of the scattering vector given in terms of wavelength of laser λ, index of refraction of the medium n and scattering angle θ by

$$q = \frac{4\pi}{\gamma} n \sin\left(\frac{\theta}{2}\right). \tag{1}$$

For a scattering angle $\theta \sim 3°$, $q \sim 0.52 \times 10^4$ cm^{-1}, and take $d \sim 1 \times 10^{-4}$ cm, we have $qd \sim 0.52$ which satisfies the criterion. Therefore for data taken at low scattering angles we can safely treat an *E. coli* as a point particle and model only its center of mass motion.

In the photon correlation technique (12) the measured photo-count correlation function is reducible to the self-correlation function

$$F_s(\mathbf{q}, t) = \langle e^{i\mathbf{q}\cdot[\mathbf{R}(t) - \mathbf{R}(0)]} \rangle \tag{2}$$

where $\mathbf{R}(t)$ and $\mathbf{R}(0)$ are, respectively, the position vectors of a typical bacterium at time t and

0, which is some arbitrarily chosen origin of time. In a homogeneous medium where motions are isotropic $F_s(\mathbf{q}, t)$ depends only on the magnitude of $\mathbf{q}$. On the other hand when motions are not isotropic, such as in the case of bacteria in a chemotactic band, $F_s(\mathbf{q}, t)$ depends on the direction of $\mathbf{q}$ vector. Let us take the direction of oxygen gradient (vertical direction) as z-direction and the direction perpendicular to it as x-direction. Then we have

$$F_{\parallel}(\mathbf{q}, t) = \langle e^{iq[z(t)-z(0)]} \rangle \tag{3}$$

$$F_{\perp}(\mathbf{q}, t) = \langle e^{iq[x(t)-x(0)]} \rangle. \tag{4}$$

Since the origin of time is arbitrary, we shall call $Z(t) \equiv z(t) - z(0)$, $X(t) \equiv x(t) - x(0)$ from now on.

Free Motion (15)

In this case we can set $Z(t) = v_z t$ for the motion in z-direction and thus

$$F_{\parallel}(\mathbf{q}, t) = \langle e^{iqv_z t} \rangle = \int_{-\infty}^{+\infty} dv_z P(v_z) e^{iqv_z t}. \tag{5}$$

It has been shown by a direct optical tracking of *E. coli* (16) in an isotropic medium that the speed distribution is closely approximated by the Maxwell distribution:

$$P(v_z) = (1/\sqrt{2\pi V_2^2}) \exp(-v_z^2/2V_2^2). \tag{6}$$

Substituting Eq. 6 into 5 we get

$$F_{\parallel}(\mathbf{q}, t) = \exp(-q^2 V_2^2 t^2/2) \tag{7}$$

From Eq. 6 we can also identify that $V_2^2 = \langle v_z^2 \rangle$. Obviously $F_{\perp}(\mathbf{q}, t)$ can also be written in the same form as Eq. 7 with $V_2^2 = \langle v_x^2 \rangle$.

This free motion approximation is good when the mean free path of the free motion L_2 is larger than q^{-1}. For example for a typical run L_2 may be 20 μm and this criterion is amply satisfied for q values at any attainable scattering angles.

B. Short Step Motion: Gaussian Approximation (7)

When the change of direction is so rapid that $qL_1 < 1$ then the motion can be modeled as a random walk of step length L_1. This is a Gaussian random process and a well known theorem (17) states

$$F_{\parallel}(\mathbf{q}, t) = \langle e^{iqZ(t)} \rangle = \exp(-q^2 \langle Z^2(t) \rangle/2) \tag{8}$$

where the mean-square displacement is given by Eq. 7

$$\langle Z^2(t) \rangle = 2L_1^2[(t/T_1) - 1 + e^{-(t/T_1)}]. \tag{9}$$

T_1 has a physical meaning of the average time duration of each small step. $V_1 = L_1/T_1$ is thus the instantaneous speed during the small step motion.

E. coli in the twiddle state can be modeled as a series of small step motions, as far as the center of mass motion is concerned. It should be noted that the Gaussian form in Eq. 8 has a nice property that

$$F_{\parallel}(\mathbf{q}, t) \xrightarrow[qL_1 \gg 1]{} \exp(-q^2 V_1^2 t^2/2) \tag{10}$$

$$F_{\parallel}(\mathbf{q}, t) \xrightarrow[qL_1 \ll 1]{} \exp(-q^2 Dt) \tag{11}$$

with $D = L_1^2/t_1$, an effective diffusion constant.

Two-State Motion

The trajectory of *E. coli* motion is composed of a sequence of motions ABABA . . . where A and B can be either run or twiddle. To model such a motion mathematically we shall adopt a stochastic approach where we regard ABABA . . . as an alternating Markovian process with certain transition probabilities. Take the case of $\mathbf{q} \parallel \hat{Z}$ for example. In a language of space-time correlations function

$$g(z, t)\mathrm{d}z = \langle \delta[z - Z(t)] \rangle \mathrm{d}z \tag{12}$$

equals a conditional probability, given that at $t = 0$ a bacterium is at $Z(0) = 0$, the bacterium will arrive at z around $\mathrm{d}z$ at $t = t$. The normalization condition for the probability demands that

$$\int_{-\infty}^{\infty} g(z, t)\mathrm{d}z = 1. \tag{13}$$

We now observe that a Fourier transform relation exists between $g(z, t)$ and $F_s(\mathbf{q}, t)$

$$F_s(\mathbf{q}, t) = \int_{-\infty}^{\infty} \mathrm{d}z\, e^{iqz} g(z, t). \tag{14}$$

We note from Eq. 14 and the definition Eq. 12 that

$$F_s(\mathbf{q}, 0) = \int_{-\infty}^{\infty} \mathrm{d}z\, e^{iqz} \delta(z) = 1. \tag{15}$$

In order to get the transition probability from one state to another, we assume that the probability of changing state during a small interval of time $(t, t + \Delta t)$ is proportional to Δt, i.e.,

$$P(t, t + \Delta t) = \frac{\Delta t}{\tau}, \tag{16}$$

From this assumption it immediately follows that the probability of a bacterium starting at $t = 0$ with a given state, will remain in the same state at time t, is given by

$$P(t) = \lim_{\Delta t \to 0} \left(1 - \frac{\Delta t}{\tau}\right)^{t/\Delta t} = e^{-(t/\tau)}. \tag{17}$$

The probability that the bacterium keeps the same state from $t = 0$ to t but makes a transition to the other state during an interval $(t, t + \Delta t)$, is then equal to

$$P(t)\frac{\Delta t}{\tau} = \frac{\Delta t}{\tau} e^{-(t/\tau)}. \tag{18}$$

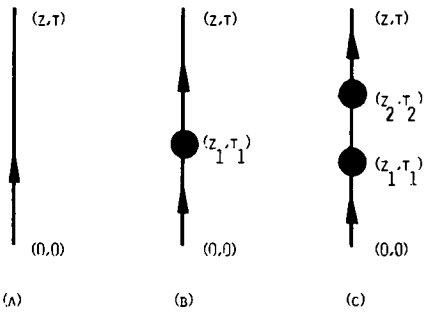

FIGURE 2 Schematic diagrams representing different terms in the stochastic model of the two-state motion. (*a*) represents terms without change of states from (0, 0) to (z, t). (*b*) represents terms with one change of state between (0, 0) and (z, t). These first-order terms are of the order (t/τ) smaller than the zeroth order term. (*c*) represents terms with two changes of states between (0, 0) and (z, t). These terms are of the order $(t/\tau)^2$, which is about 0.04 of the zeroth order terms, and therefore are neglected.

This exponentially decaying probability seems to be well confirmed by Berg and Brown's experiment (18).

We are now ready to write down the compound process of ABABA . . . in terms of these basic probabilities. We shall call the twiddle state by *1* and the run state by *2*.

ZEROTH ORDER PROCESS There is no change of state from (0, 0) to (z, t). (See Fig. 2 *a*)

$$g^{(0)}(z, t) = \frac{\tau_1}{\tau_1 + \tau_2} P_1(t) g_1(z, t) + \frac{\tau_2}{\tau_1 + \tau_2} P_2(t) g_2(z, t). \tag{19}$$

FIRST ORDER PROCESS There is one change of state between (0, 0) and (z, t). (See Fig. 2 *b*).

$$g^{(1)}(z, t) = \frac{\tau_1}{\tau_1 + \tau_2} \int_0^t dt_1 \int_{-\infty}^{\infty} dz_1 P_2(t - t_1) g_2(z - z_1, t - t_1) \left(\frac{1}{\tau_1}\right) P_1(t_1) g_1(z_1, t_1)$$

$$+ \frac{\tau_2}{\tau_1 + \tau_2} \int_0^t dt_1 \int_{-\infty}^{\infty} dz_1 P_1(t - t_1) g_1(z - z_1, t - t_1) \left(\frac{1}{\tau_2}\right) P_2(t_1) g_2(z_1, t_1) \tag{20}$$

$$= \frac{2}{\tau_1 + \tau_2} \int_0^t dt_1 \int_{-\infty}^{\infty} dz_1 P_1(t - t_1) g_1(z - z_1, t - t_1) P_2(t_1) g_2(z_1, t_1). \tag{21}$$

Eq. 21 follows from 20 because two terms in Eq. 20 can be shown to be identical by a simple change of space and time variables. The various notations used are summarized as follows: τ_1 is the average duration of twiddle motion; note $\tau_1 > T_1$, $L_1 = V_1 T_1$. τ_2 is the average duration of run motion;

$$P_1(t) = \exp(-t/\tau_1) \tag{22}$$

$$P_2(t) = \exp(-t/\tau_2). \tag{23}$$

$g(z, t)$ is the conditional probability function defined in Eq. 12 while subscripts 1 and 2 refer, respectively, to the twiddle and run correlation functions. The final result is

$$g(z, t) = g^{(0)}(z, t) + g^{(1)}(z, t) + g^{(2)}(z, t) + \cdots \tag{24}$$

If the observation time t (time scale of the correlation function measured) is small compared with both τ_1 and τ_2 then during the observation the majority of bacteria can make at most only one transition. We shall show later that this is the case for our experiment. We can therefore safely neglect the higher order terms $g^{(2)}(z, t)$, etc. From the Eqs. 14 and 24, the self-correlation function can then be written as

$$F_s(\mathbf{q}, t) = \frac{\tau_1}{\tau_1 + \tau_2} P_1(t) F_1(\mathbf{q}, t) + \frac{\tau_2}{\tau_1 + \tau_2} P_2(t) F_2(\mathbf{q}, t) + \frac{2}{\tau_1 + \tau_2} \int_0^t dt_1 P_1(t - t_1) P_2(t_1) F_1(\mathbf{q}, t - t_1) F_2(\mathbf{q}, t_1) \quad (25)$$

where from the discussions of Free and Short Step Motion we should put

$$F_1(\mathbf{q}, t) = \exp\left[-q^2 L_1^2 \left(\frac{t}{T_1} - 1 + e^{-(t/T_1)}\right)\right] \quad (26)$$

$$F_2(\mathbf{q}, t) = \exp\left[-q^2 V_2^2 t^2/2\right]. \quad (27)$$

Note that Eq. 25 satisfies the condition Eq. 15, $F_s(\mathbf{q}, 0) = 1$. From Eq. 25, we can see that the third term is 0 (t/τ) of the first and the second term where τ is either τ_1 or τ_2.

Exactly the same formulae are obtained for the case $\mathbf{q} \parallel \hat{x}$, just by replacing all the z in the formula by x.

Mean-Square Displacement

It is easy to see from Eq. 14 that once the analytic form of $F_s(\mathbf{q}, t)$ is obtained, the mean-square displacement can be calculated by putting

$$\left[-\frac{\partial^2}{\partial q^2} F_s(\mathbf{q}, t)\right]_{q=0} = \langle Z^2(t) \rangle \text{ or } \langle X^2(t) \rangle. \quad (28)$$

Using expression $F_s(\mathbf{q}, t)$ in Eq. 25 we get

$$\langle Z^2(t) \rangle = \frac{\tau_1}{\tau_1 + \tau_2} P_1(t) W_1(t) + \frac{\tau_2}{\tau_1 + \tau_2} P_2(t) W_2(t) + \frac{2}{\tau_1 + \tau_2} \int_0^t dt_1 P_1(t - t_1) P_2(t_1) [W_1(t - t_1) + W_2(t_1)] \quad (29)$$

where

$$W_1(t) = 2L_1^2 \left(\frac{t}{T_1} - 1 + e^{-(t/T_1)}\right) \quad (30)$$

$$W_2(t) = V_2^2 t^2. \quad (31)$$

Especially as $t \to 0$

$$\langle Z^2(t) \rangle \xrightarrow[t \to 0]{} [\beta V_1^2 + (1 - \beta) V_2^2] t^2 \quad (32)$$

where

$$V^2 = \beta V_1^2 + (1 - \beta) V_2^2 \tag{33}$$

is the mean-square speed of the center of mass and

$$\beta = \frac{\tau_1}{\tau_1 + \tau_2} \tag{34}$$

is the fraction of time the bacterium spend in the twiddle state. We observe here that the final expression for the self-correlation function Eq. 25 is a short time approximation. A time domain technique such as the photon correlation spectroscopy has a definite advantage in this type of experiment. For the frequency domain technique which measures the time Fourier transform $S_s(\mathbf{q}, w)$ of $F_s(\mathbf{q}, t)$ one would have to calculate an infinite sum of $g^{(n)}(z, t)$.

EXPERIMENTAL RESULTS AND DISCUSSION

General Description

Because we are interested in studying motions of bacteria at different portions of the chemotactic band where they are subjected to different oxygen concentration gradients, we chose scattering at a fixed small forward angle. The fast and automatic data processing ability of our spectrometer system allows repetitive accumulations of many correlation functions as the chemotactic band moves through the laser beam. For a 1-mm thick band, migrating at speed 0.85 m/s and with one loop of data processing time of 2 min and 30 s, correlation functions can be accumulated at ten or more different sections of the band. Thus, spatial resolution of the experiment is ~100 μm. It is considerably larger than mean free path of a bacterial run which is <50 μm. In order to study anisotropic motions along and perpendicular

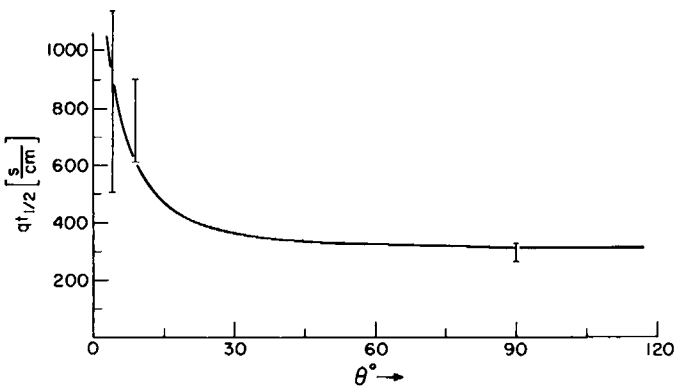

FIGURE 3 Halfwidths of the normalized self-correlation functions $F_s(\mathbf{q}, t)$ for scattering angles 3.72°, 8.67° and 90°. The vertical range at each angle shows the variation of the halfwidth at different parts of the band. The solid line is calculated according to a model from experiment I of twiddling and running bacteria as $F_s(q, t) = \beta F_1(q, t) + (1 - \beta)F_2(q, t)$ with parameters: $V_2 = 22$ μm/s, speed of running bacteria; $L_1 = 0.13$ μm, step length of jitter motion; and $\beta = 0.67$, the average fraction of twiddling bacteria at given time.

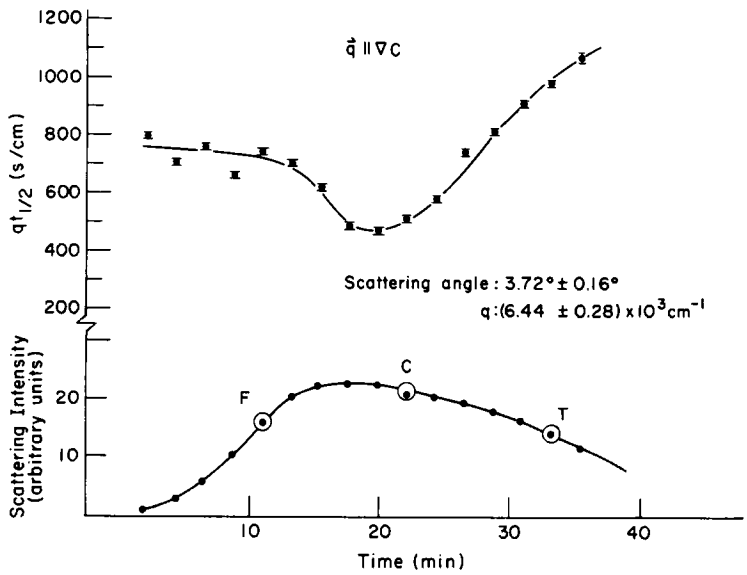

FIGURE 4 Scaled halfwidths of the self-correlation functions at different locations in a chemotactic band. The top curve is the scaled halfwidth and the bottom curve the band profile. The scattering vector was chosen to be parallel to the direction of the oxygen concentration gradient. Notice the halfwidth becomes smaller at the center part of the band. Three representative locations (Front, Center, Tail) in the band are chosen for further detailed analysis later.

to the oxygen concentration gradient, two scattering vectors were chosen, a parallel one with q equal to 0.644 μm^{-1}, and a perpendicular one with q equal to 1.50 μm^{-1}. Measurements were also made at 90° scattering angle in order to compare the result with that reported in experiment I. Several bands have been studied at different dates. A band usually lasts for ~5 h. Within this period two or three series of measurements can be made. All data showed essentially the same qualitative behavior. Two complete sets of data in particular were analyzed in detail, out of which we present only one set of the results in the following.

Halfwidths of the self-correlation functions taken at different scattering angles are plotted in Fig. 3. The bars indicated the range of halfwidth of the self-correlation functions at different sections of the band for each case. The solid line is the result taken from experiment I which represents the width of the correlation functions averaged over the whole band. It is seen that the agreement is good, indicating that the bacterial motility in these two cases is about the same. In Figs. 4–6, the scaled halfwidth of the correlation function is plotted at each location of the band profile. Fig. 4 is the parallel case at θ angle equal to 3.72°. The upper curve is the scaled halfwidth and the lower curve represents the band profile. It is to be remembered that the band migration speed is ~0.8 $\mu m/s$, which means that a 20-min time scale in the x-axis corresponds to ~1 mm. Notice that the halfwidth becomes appreciably smaller toward the center of the band. We shall analyze later three correlation functions specifically denoted as front, center, and tail. Fig. 5 is the perpendicular case at $\theta = 8.67°$. In contrast to the parallel case the scaled halfwidth is rather constant throughout the band. At first glance, one might think the narrowing of the halfwidth at parallel case is due to a greater velocity at the center of the band. However, it turns out that it is mainly due to the fact that

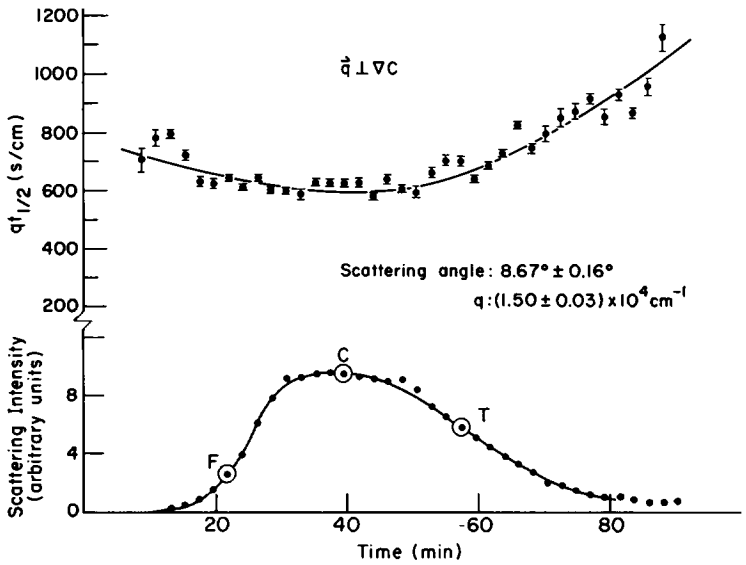

FIGURE 5 Scaled halfwidths of the self-correlation functions at different locations in a chemotactic band. The scattering vector was chosen to be perpendicular to the direction of the oxygen concentration gradient. Notice the halfwidths remain rather constant throughout the band. Three representative locations (Front, Center, Tail) in the band are chosen for further detailed analysis later.

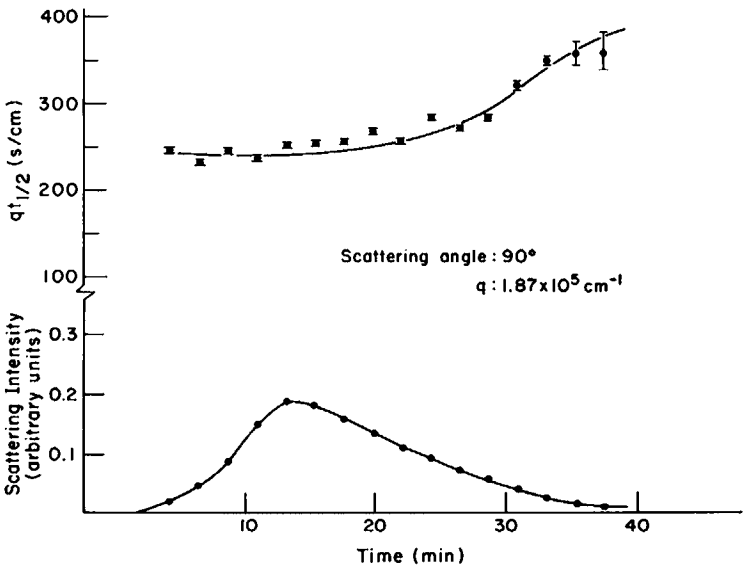

FIGURE 6 Scaled halfwidths of the self-correlation functions at different locations in a chemotactic band. The scattering angle was 90°. The scattering vector was perpendicular to the direction of the oxygen concentration gradient. Notice the halfwidths remain nearly constant throughout the band.

the fraction of bacteria in the twiddle state at the center of the band is much less than that in the front and the tail part of the band. The run speed at the center of the band in the parallel case is about the same as it is in the perpendicular case. Fig. 6 shows results taken at 90° scattering angle. The scaled halfwidth is fairly constant throughout the band as in the perpendicular case and increases gradually towards the tail of the band. This is probably due to some lower motility bacteria lagging behind as band moves upward. It should be noted that the halfwidth at 90° is at the level of 250 s/cm while in both parallel and perpendicular cases the level is at ~600 s/cm. This difference is due to the effect of twiddle, which becomes important at small angles as observed in experiment I.

Data Analysis According to Two-State Model

The correlation functions taken at small angles all show the following general features. At short time it decays like a Gaussian function, but at the intermediate range like a simple exponential and then follows with a long tail. This clearly indicates that it requires a model that contains terms behaving like a free motion, a small step motion, and a transition between them, respectively. A stochastic model for the two-state motions described in the section Theory: Two-state Motion contains just such ingredients. From Eq. 25, the self-correlation function contains five independent parameters: T_1 (average time step for small step motion), L_1 (average step length for small step motion), τ_1 (duration of twiddle), τ_2 (duration of run), and V_2 (averaged speed of run). Among them V_2 and β ($\beta = \tau_1/(\tau_1 + \tau_2)$) are the most interesting quantities, as far as chemotaxis is concerned. The purpose of the data analysis is to try to obtain these two parameters at different portions of the band for both parallel and perpendicular cases.

A computer program was written for MINC/11 minicomputer (Digital Equipment Corp. Maynard, Mass.) which evaluates the three-terms expression of Eq. 25. A theoretical correlation function is then compared with experimental points. Input data points are taken from every fifth channel by a five point average of neighboring points. The channel width is uniformly 2 ms, so data points are separated by 10 ms. The effective time range of the correlation function fitted is about 100 channels or 0.2 s. The good fit is judged by χ^2 where

$$\chi^2 \equiv \sum_i \frac{(\text{theory} - \text{data})_i^2}{(\text{theory})_i}. \tag{35}$$

It is found that all six sets of data can be fitted with the same parameter L_1, which is consistent with a requirement that $q_0 L_1 \sim 1$. q_0 corresponds to the scattering vector at the angle where the scaled halfwidth begins to rise steeply in Fig. 3. This corresponds to a physical picture that $1/q_0$ is approximately the step length L_1 which works out to be 0.3 μm. With L_1 fixed at this value, it is also found that a choice of T_1, can be narrowed down to a range 0.013–0.02 s. The main feature of the correlation function seems to be determined mostly by two key parameters V_2 and β. We choose to keep τ_1 constant at 0.43 s which produces an overall fit to all the curves with $\chi^2 < 0.1\%$.

In Fig. 7, the self-correlation function at the front, center and tail part of both parallel and perpendicular cases is plotted as a function of universal scale qVt. The experimental data are the dots along the fitted curve and the best fitted parameter for each case is indicated on each graph. The dashed lines 1, 2, and 3 in the parallel and perpendicular front cases are the

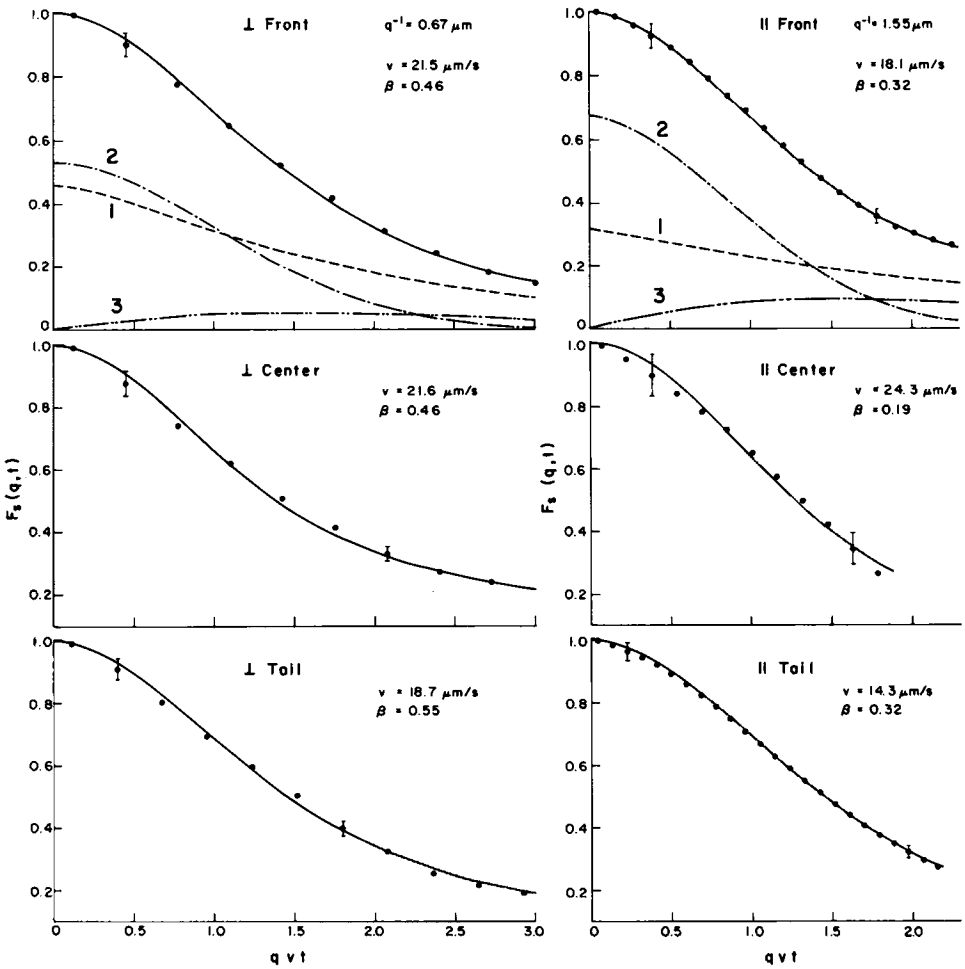

FIGURE 7 Fitted self-correlation functions for the front, center, and tail of the parallel and perpendicular cases. The self-correlation functions are plotted as function of a universal time scale of qVt. V is an average center of mass speed $V = [\beta V_1^2 + (1-\beta)V_2^2]^{1/2}$. The dots are experimental data and solid lines are theoretical curves obtained with parameters listed in Table I. Curve *1* denotes the contribution from twiddle. Curve *2* denotes the contribution from run. Curve *3* represents contribution from transitions from twiddle to run and vise versa. The effective range of the self-correlation function is ~100 channels or 0.2 s.

contributions from the first, second, and third term in Eq. 25, respectively. The contribution of run mainly comes in at the front part of the self-correlation function. At the tail, contribution from twiddle is dominant. The contribution of the changing state term is insignificant for very short times. It rises to a small (10%) contribution as times goes on and then gradually dies out at long times. The best-fit parameters for all cases are summarized in Table I. In principle if we have an accurate correlation function which extends to sufficiently long times it is possible to obtain a unique set of the five parameters. In practice owing to a relatively short accumulation time of the correlation function (2 min) there is a certain amount of statistical uncertainty in the data points, especially at the tail of the correlation function. This

TABLE I
MOTIONAL PARAMETERS OF *E. coli* (K12, WILD TYPE) IN OXYGEN GRADIENT OBTAINED BY THE RUN-TWIDDLE ANALYSIS

Position	V	T_1	L_1	τ_1	τ_2	β	V_2	χ^2
	(μm/s)	*(s)*	*(μm)*	*(s)*	*(s)*		*(μm/s)*	*(%)*
Parallel Case (q^{-1} = 1.55 μm)								
Front	18.1	0.02	0.3	0.43	0.92	0.32	19.4	0.14
Center	24.3	0.02	0.3	0.43	1.80	0.19	26	1.09
Tail	14.3	0.02	0.3	0.43	0.92	0.32	14	0.24
Perpendicular Case (q^{-1} = 0.67 μm)								
Front	21.5	0.013	0.3	0.43	0.5	0.46	20	0.29
Center	21.6	0.02	0.3	0.43	0.5	0.46	26	0.49
Tail	18.7	0.017	0.3	0.43	0.35	0.35	20	0.55

uncertainty constrains us in general to the analysis of data points up to 100 channels ($t \leq 0.2$ s). Since τ_1 and τ_2 are in the range of 0.35–1.8 s, the correlation functions used are not long enough to allow the two exponential functions $P_1(t)$ and $P_2(t)$ to influence the correlation function appreciably. This means that it is difficult to determine τ_1 and τ_2 individually accurately in the fitting process. Nevertheless the important parameter β, which is related to the ratio τ_1/τ_2, can be determined fairly reliably, because it enters the first and second term in Eq. 25 multiplicatively. Furthermore, it is perhaps not appropriate to compare parameters in the parallel and perpendicular cases quantitatively because the two sets of measurements were made consecutively 2 h apart. During this relatively long time period the chemotactic ability of the bacteria might have changed. However, in each case comparison of parameters at different portions of the band should be meaningful. We would like to draw attention to the parallel center case: β is 0.19 which is very different from a value of 0.32 at both the front and tail of the band. The average running time is 1.8 s which is two times larger and the speed of the run is also larger than it is on both sides. In contrast, for the perpendicular case, β is essentially independent of the position in the band. The run speed though is substantially larger compared to the sides. It is the same as the speed at the center of the band in the parallel case. A larger β value is observed in the perpendicular case, as compared to the parallel case. This may be due to the fact that the bacteria have lost some of their chemotactic ability.

These fitted parameters are similar to what Berg and Brown have observed (18), even though in their experiment serine instead of oxygen was used as an attractant. In their results, τ_2, the average running time up and down the gradient is 1.80 s, the same as in our case. In a homogeneous solution their average run time is 0.83 s while in our case the average run time in the front and tail is 0.92 s for both. At the front and tail, oxygen concentration gradient is low so bacteria sense almost a homogeneous medium.

We would like to add a word of caution, here. Although the choice of $\tau_1 = 0.43$ s gave us excellent fits to all curves, it is also possible to get an over-all fit to all curves with a slight increase in χ^2, by choosing a different value of τ_1. For example, we have tried $\tau_1 = 0.14$ s, an average twiddle duration which is observed by Berg and Brown (18) in the serine case. With

this choice, τ_2 in the parallel center turns out to be 0.59 s and on both sides of it, 0.27 s. The β values obtained are 0.19 and 0.34, respectively, which are exactly the same as before. We have also tried many other combinations and our conclusion is as follows. Because of the finite length and accuracy of the correlation functions values of τ_1 and τ_2 are not uniquely determined by the fitting. However, their ratio, or β values obtained are rather unique. Thus, if one can fix τ_1 based on other criteria then τ_2 can be determined. We also observed that the average run speed V_2 can be determined uniquely.

Using Eq. 29 and the best-fit parameters from the front in both parallel and perpendicular cases, we can compute the average displacement along $\hat{z}$ direction or $\hat{x}$ direction. The results are plotted in Fig. 8. This is a very interesting plot because it gives an intuitive picture of how a bacterium moves in either $\hat{x}$ or $\hat{z}$ direction. With the same run speed in both parallel and perpendicular cases, just because β are different, the average displacement in $\hat{z}$-direction can be 1.3 times longer than it is in $\hat{x}$-direction after 0.2 s. This illustrates well how chemotaxis is a result of changing β.

By fitting $F_s(\mathbf{q}, t)$ and $-(2/q^2) \ln F_s(\mathbf{q}, t)$ to a t^2 function at short time, we can estimate the average center of mass speed V. This value can be used to set the initial value of speed in the data fitting process. Fig. 9 shows that the averaged speeds derived from this method are 18.0 μm/s and 15.0 μm/s for the front and tail part of the parallel case, respectively.

CONCLUSION

In this paper we have presented a new technique of measuring important chemotaxis parameters β and V_2 using photon correlation spectroscopy. By choosing to do scattering experiments at small angle, we minimize the complications due to nonspherical shape and structural effects of bacteria. At small enough scattering angle, even the effect of wobbling (rotation) during the run can be made to be negligible (9). Thus only the center of mass

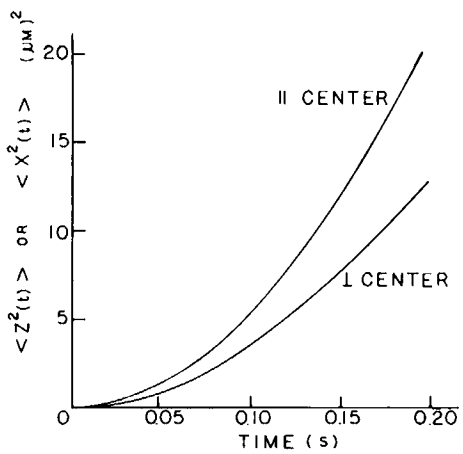

FIGURE 8 Computed mean-square displacement $\langle Z^2(t) \rangle$ [or $\langle X^2(t) \rangle$] of the *E. coli* in the direction of (or in the direction perpendicular to) oxygen concentration gradient. The mean-square displacements at the center of the band are plotted according to the best-fit parameters. Notice that at $t = 0.2$ s. the bacterium reaches 4.6 μm in the parallel case and 3.6 μm in the perpendicular case.

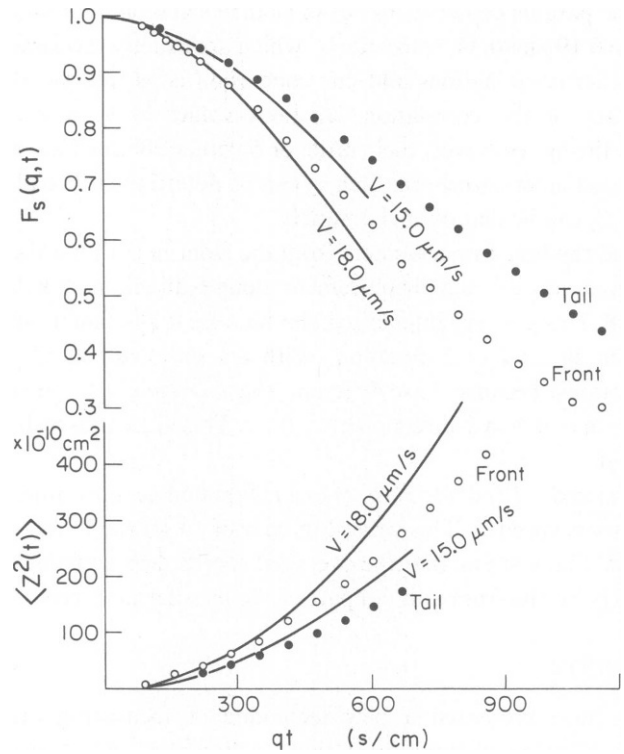

FIGURE 9 Short time parts of normalized self-correlation functions (in parallel geometry) at the front and tail part of the migrating band. The solid curves are best fits to a functional form $F_s(q, t) = \exp(-\frac{1}{2} q^2 V^2 t^2)$. Black dots ● and open circles ○ are the experimental values. The bottom graphs are the experimental mean-square displacement at short time obtained by calculating $\langle z^2(t) \rangle = -(2/q^2) \ln F_s(\mathbf{q}, t)$. The solid curves are calculated from $\langle Z^2(t) \rangle = V^2 t^2$.

motion need to be taken into account. Furthermore, because the small step motion (twiddle) contributes significantly to the correlation function only at small q ($q < q_0$) one has a good sensitivity to study the important chemotaxis parameters. By choosing $\mathbf{q}$ vectors parallel and perpendicular to the chemical gradient we are then able to see the anisotropic motion of bacteria in chemotaxis. Although in parallel geometry motion is not symmetrical along and opposite to the gradient, light scattering cannot distinguish between these two motions. Thus measured parameters are averages between these two directions. The asymmetry between $\langle Z^2(t) \rangle$ and $\langle X^2(t) \rangle$ as shown in Fig. 8 is a short time behavior. The theory as it is written down is only capable of describing bacterial motions during an interval of time <0.2 s. The observed band propagation with a drift velocity of 0.85 μm/s is a much longer time phenomenon which this theory is incapable of describing. In this theory motions of bacteria up and down the gradient are taken to be symmetric and therefore the drift velocity is zero. In practice with $V_2 \simeq 26$ μm/s and $V_{\text{drift}} \simeq 0.85$ μm/s, so this idealization is not unreasonable.

A new contribution in the present paper is the development of an improved theory by which one is in principle able to extract all the relevant parameters. The improvement of the present theory over that in experiment I is in the incorporation of the third term in Eq. 25. The theory as described in experiment I is applicable only in the limiting case that both τ_1 and τ_2 are

much longer than the observation time t. However, the experimental situation is such that this is not quite the case as can be seen from Table I. In this sense, the present theory is a much better approximation to the real situation.

We have demonstrated the applicability of this technique only in the case of oxygen in this paper because of its simplicity of interpretation. Our further plan is to extend the same experiment to a more interesting case of using serine as an attractant.

This work is supported by a National Science Foundation grant no. PCM-7815844.

Received for publication 2 January 1981 and in revised form 8 April 1981.

REFERENCES

1. MacNab, R. M., and D. E. Koshland, Jr. 1972. The gradient sensing mechanism in bacterial chemotaxis. *Proc. Natl. Acad. Sci. U. S. A.* 60:2509.
2. Berg, H. C., and D. A. Brown. 1972. Chemotaxis in *Escherichia coli* analyzed by three-dimensional tracking. *Nature (Lond.).* 239:500.
3. Adler, J. 1975. Chemotaxis in bacteria. *Annu. Rev. Biochem.* 44:341.
4. Berg, H. C. 1975. Chemotaxis in bacteria. *Annu. Rev. Biophys. Bioeng.* 4:119.
5. Koshland, D. E., Jr. 1977. A response regulator model in a simple sensory system. *Science (Wash. D.C.).* 196:1055.
6. Adler, J. 1966. Chemotaxis in bacteria. *Science (Wash. D.C.).* 153:708.
7. Holz, M., and S. H. Chen. 1978. Quasi-elastic light scattering from migrating chemotactic bands of *Escherichia coli. Biophys. J.* 23:15.
8. Stock, G. B., and F. D. Carlson. 1975. Photon autocorrelation spectra of wobbling and translating bacteria. *In* Swimming and Flying in Nature. Y. T. Wu, C. J. Brokaw, and C. Brennan, editors. Plenum Press. 1:57.
9. Holz, M., and S. H. Chen. 1978. Rotational-translational models for interpretation of quasi-elastic light scattering spectra of motile bacteria. *Appl. Opt.* 17:3197.
10. Holz, M., and S. H. Chen. 1978. Structural effects in quasi-elastic light scattering from motile bacteria of *E. coli. Appl. Opt.* 17:1930.
11. Adler, J., and B. Templeton. 1967. The effect of environmental conditions on the motility of *Escherichia coli. J. Gen. Microbiol.* 46:175.
12. Chen, S. H., and W. B. Veldkamp, and C. C. Lai. 1975. Simple digital clipped correlator for photon correlation spectroscopy. *Rev. Sci. Instrum.* 46:1356.
13. Kotlarchyk, M., S. H. Chen, and Shoji Asano. 1979. Accuracy of RGD approximation for computing light scattering properties of diffusing and motile bacteria. *Appl. Opt.* 18:2470.
14. Chen, S. H., M. Holz, and P. Tartaglia. 1977. Quasi-elastic light scattering from structured particles. *Appl. Opt.* 16:187.
15. Nossal, R., S. H. Chen, and C. C. Lai. 1977. Use of laser scattering for quantitative determinations of bacterial motility. *Opt. Comm.* 4:35.
16. Holz, M., and S. H. Chen. 1978. Tracking bacterial movements using a one-dimensional fringe system. *Opt. Lett.* 2:109.
17. Chandrasekhar, S. 1943. Stochastic problems in physics and astronomy. *Rev. Mod. Phys.* 15:1.
18. Berg, H. C., and D. A. Brown. 1974. Chemotaxis in *Escherichia coli* analyzed by three-dimensional tracking. *Antibiot. Chemother.* 19:55–58.